THE JOURNAL OF PHYSICAL CHEMISTRY B

Article

pubs.acs.org/JPCB

Membrane Interacting Regions of Dengue Virus NS2A Protein

Henrique Nemésio and José Villalaín*

Molecular and Cellular Biology Institute, Universitas "Miguel Hernández", E-03202 Elche-Alicante, Spain

Supporting Information

ABSTRACT: The Dengue virus (DENV) NS2A protein, essential for viral replication, is a poorly characterized membrane protein. NS2A displays both protein/protein and membrane/protein interactions, yet neither its functions in the viral cycle nor its active regions are known with certainty. To highlight the different membrane-active regions of NS2A, we characterized the effects of peptides derived from a peptide library encompassing this protein's full length on different membranes by measuring their membrane leakage induction and modulation of lipid phase behavior. Following this initial screening, one region, peptide dens25, had interesting effects on membranes; therefore, we sought to thoroughly characterize this region's interaction with membranes. This peptide presents an interfacial/hydrophobic pattern characteristic of a membrane-proximal segment. We show that dens25 strongly interacts with membranes that contain a large proportion of lipid molecules with a formal negative charge, and that this effect has a major electrostatic contribution. Considering its membrane modulating capabilities, this region might be involved in membrane rearrangements and thus be important for the viral cycle.

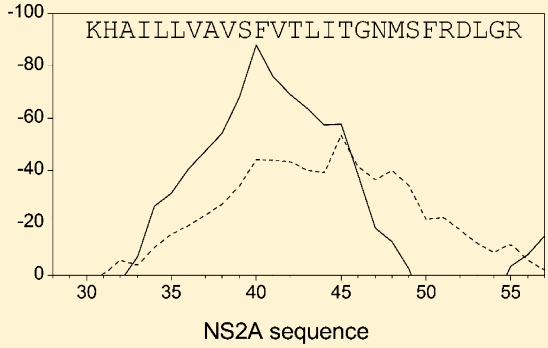

INTRODUCTION

There are three genera in *Flaviviridae*, *Flavivirus*, *Hepacivirus*, and *Pestivirus*.[1] Dengue virus (DENV) and several other highly pathogenic viruses like the Tick-borne encephalitis virus (TBEV) or the Yellow Fever virus (YFV) are part of the *Flavivirus* genus. For the best part of the last century, Dengue virus has been the most prevalent arbovirus affecting the human population. Once restricted to the tropics and subtropics, it is now spreading to previously unaffected zones, owing to the dispersion of its vectors, *Aedes* spp., driven by several factors, among them an ever-increasing global temperature and widespread traveling. Apart from that, the fact that the last year there were over 390 million estimated cases,[2] DENV is becoming a serious threat to public health. Although the most common clinical manifestations are asymptomatic or mild fevers that can be tackled with well-equipped hospitals, there are two other serious life threatening situations with mortality rates surpassing 20% if left unattended.[3] The fact that more than 40% of the world population lives in regions where Dengue vectors thrive, leaving close to 3 billion people at risk in the world, should not be overlooked.[4] Although several compounds have been identified to inhibit DENV replication,[5] there is actually no clinical treatment for its infection.

The DENV viral genome consists of a single strand of positive RNA that contains a single open reading frame, encoding a polyprotein of more than 3000 residues. After cleavage and maturation by several proteases, this protein gives rise to three structural and seven nonstructural proteins.[6] Similarly to other enveloped viruses, DENV enters the cells via receptor mediated endocytosis through clathrin coated pits.[6−9] Once inside the cell, its proteins rearrange cellular membranes that ultimately result in the formation of unique structures where the replication complexes are located.[10−12] A significant part of its viral cycle remains elusive, yet its proteins take part in protein−protein and protein−lipid interactions in a very intricate manner.[6,9] Throughout all of its viral cycle, DENV is associated with membranes and all of its essential steps take place in membranes, especially endoplasmic reticulum (ER) membranes. Although the specific genome encapsulation, virion formation, and fusion processes are widely accepted to be almost exclusively carried through by the structural proteins C, prM, and class II fusion protein E, much is still being debated about the exclusivity of those proteins in those processes.[13−15]

All the polyprotein processing and viral RNA replication steps are generally assigned to the nonstructural proteins, including the formation of replication complexes of the virus.[16] The accumulated knowledge on the functions of NS1, NS2A, NS4A, and NS4B on the viral cycle is very sparse, mainly due to their considerable hydrophobicity and the difficulty of discerning their exact roles.[17] NS4A and NS4B seem to be involved in the host's immune system evasion and immune response, affecting several pathways.[18,19] Protein NS1 is found mainly in the cytosol of the cell, rendering it an ideal antigen for DENV infection detection, and seems to play a role in autophagy as well.[20] One of the proteins found in the replication complex of flaviviruses is NS2A,[16] what would certify its role in the viral replication. This protein is required for the proper processing of NS1, possesses specific recognition

Received: May 19, 2014
Revised: August 2, 2014
Published: August 13, 2014

   dx.doi.org/10.1021/jp504911r | J. Phys. Chem. B 2014, 118, 10142−10155

sites for certain proteases, is also involved in the interferon inhibition by NS4A and NS4B, and is mainly found in ER membranes.[18,21,22] Recently, a topology model was proposed where NS2A is described as having one N-terminal segment from residues 1 to 31 with no described membrane interaction, followed by a segment, residues 32−68, that despite lacking the ability to traverse the membrane is proposed to be in close association with it.[23] Two transmembrane segments ensue from residues 69 to 119, followed by a non-transmembrane segment from residues 120 to 142, and ending with three transmembrane segments from residues 143 to 209.

We have resorted to a set of biophysical methods used extensively in our laboratory[24−31] that allow the screening of membrane interacting regions from viral proteins. We sought to highlight regions that could be important for proper NS2A function, since this protein, essential in the viral RNA replication process, is a poorly characterized highly hydrophobic protein that requires the membrane to perform its functions. Furthermore, DENV protein/lipid and protein/protein interactions are thought to be therapeutic targets for DENV infection. From both of those points, we sought to highlight the membrane-active regions of this protein, identifying several regions with different interacting capabilities. Besides, we characterize a NS2A peptide, peptide dens25, with interesting properties on membranes. We resorted to several biophysical techniques, such as fluorescence spectroscopy, differential scanning calorimetry (DSC), and Fourier transform infrared spectroscopy (FTIR), using several model membrane systems. These results possibly provide new therapeutic targets needed to develop new strategies to thwart this highly worrying public health problem.

MATERIALS AND METHODS

Materials and Reagents. A set of 35 peptides encompassing the full length of Dengue Virus Type 2 NGC NS2A protein (Table 1) was provided by BEI Resources, National Institute of Allergy and Infectious Diseases, Manassas, VA, USA. Peptides were solubilized with H_2O/2,2,2-trifluoroethanol at a 70:30 ratio (v/v). The peptides had a purity of about 80%. The peptide dens25 corresponding to the sequence[30]KHAILLVALLVAVSFVTLITGNMSFRDLGR[55] from Dengue Virus Type 2 NGC NS2A protein (with N-terminal acetylation and C-terminal acetylation) and a purity greater than 95% was obtained from Genemed Synthesis, San Antonio, TX, USA. To prevent the infrared interference of residual trifluoroacetic acid at around 1673 cm^{-1},[32] the peptide sample was subjected to at least three lyophilization/solubilization steps in 10 mM hydrochloric acid.[33] Bovine brain phosphatidylserine (BPS), bovine liver L-α-phosphatidylinositol (BPI), cholesterol (Chol), egg phosphatidic acid (EPA), egg L-α-phosphatidylcholine (EPC), egg L-α-phosphatidylglycerol (EPG), egg sphingomyelin (ESM), egg trans-sterified L-α-phosphatidylethanolamine (TPE), tetramyristoyl cardiolipin (CL), liver lipid extract, bis(monomyristoylglycero)phosphate (BMP), 1,2-dimyristoilphosphatidylcholine (DMPC), 1,2-dimyristoylphosphatidylglycerol (DMPG), 1,2-dimyristoylphosphatidylserine (DMPS), 1,2-dimyristoylphosphatidic acid (DMPA), and 1,2-dielaidoyl-*sn*-glycero-3-phosphatidylethanolamine (DEPE) were purchased from Avanti Polar Lipids (Alabaster, AL, USA). The composition of the synthetic endoplasmic reticulum was EPC/CL/BPI/TPE/BPS/EPA/SM/Chol in the following proportion 59:0.37:7.7:18:3.1:1.2:3.4:7.8.[34,35] According to the manufacturer, the liver lipid extract contains 42% phosphatidylcholine, 22% phosphatidylethanolamine, 7% Chol, 8% phosphatidylinositol, 1% lysophosphatidylinositol, and 21% miscellaneous lipids including neutral ones. 5-Carboxyfluorescein (CF, >95% by HPLC), deuterium oxide (99.9% by atom), Triton X-100, EDTA, and HEPES were acquired from Sigma-Aldrich (Madrid, Spain). 1,6-Diphenyl-1,3,5-hexatriene (DPH) and *N*-(fluorescein-5-thiocarbamoyl)-1,2-dihexadecanoyl-*sn*-glycero-3-phosphoethanolamine (fluorescein DHPE or FPE) were acquired from Molecular Probes (Eugene, OR, USA). Every other reactant was obtained in its purest form from Sigma-Aldrich (Madrid, Spain). Deionized water was distilled twice and passed through a Milli-Q apparatus (Millipore Ibérica, Madrid, Spain) to a resistivity higher than 18 MΩ·cm.

Table 1. Sequence and Residue Position of the Peptides Contained in the DENV2 NS2A Derived Peptide Library[a]

peptide	amino acid sequence	sequence	length	net charge
1	GHGQIDNFSLGVLGMAL	1−17	17	−1
2	NFSLGVLGMALFLEEML	7−23	17	−2
3	LGMALFLEEMLRTRVGT	13−29	17	0
4	LEEMLRTRVGTKHAILL	19−35	17	+1
5	TRVGTKHAILLVAVSFV	25−41	17	+2
6	HAILLVAVSFVTLITGN	31−47	17	0
7	AVSFVTLITGNMSFRDL	37−53	17	0
8	LITGNMSFRDLGRVMVM	43−59	17	+1
9	SFRDLGRVMVMVGATMT	49−65	17	+1
10	RVMVMVGATMTDDIGMG	55−71	17	−1
11	GATMTDDIGMGVTYLAL	61−77	17	−2
12	DIGMGVTYLALLAAFKV	67−83	17	0
13	TYLALLAAFKVRPTFAA	73−89	17	+2
14	AAFKVRPTFAAGLLLRK	79−95	17	+4
15	PTFAAGLLLRKLTSKEL	85−101	17	+2
16	LLLRKLTSKELMMTTIG	91−107	17	+2
17	TSKELMMTTIGIVLLSQ	97−113	17	0
18	MTTIGIVLLSQSTIPET	103−119	17	−1
19	VLLSQSTIPETILELTD	109−125	17	−3
20	TIPETILELTDALALGM	115−131	17	−3
21	LELTDALALGMMVLKMV	121−137	17	−1
22	LALGMMVLKMVRKMEKY	127−143	17	+3
23	VLKMVRKMEKYQLAVTI	133−149	17	+3
24	KMEKYQLAVTIMAILCV	139−155	17	+1
25	LAVTIMAILCVPNAVIL	145−161	17	0
26	AILCVPNAVILQNAWKV	151−167	17	+1
27	NAVILQNAWKVSCTILA	157−173	17	+1
28	NAWKVSCTILAVVSV	163−177	15	+1
29	VSCTILAVVSVSPLFLT	167−183	17	0
30	AVVSVSPLFLTSSQQKA	173−189	17	+1
31	PLFLTSSQQKADWIPLA	179−195	17	0
32	SQQKADWIPLALTIKGL	185−201	17	+1
33	WIPLALTIKGLNPTAIF	191−207	17	+1
34	TIKGLNPTAIFLTTLSR	197−213	17	+2
35	PTAIFLTTLSRTNKKR	203−218	16	+4

[a]The sequence of peptide dens25, KHAILLVAVSFVTLITGNMSFRDLGR, is underlined. See text for details.

Vesicle Preparation. Aliquots with previously quantified formulations and dissolved in a 2:1 (v/v) chloroform to methanol solution were put under a stream of O_2-free N_2 to evaporate the solvent and then put under a vacuum protected from light for over 3 h to ensure no traces of solvent remained. To obtain multilamellar vesicles (MLVs), resuspended lipid

samples were incubated at either 25 or 10 °C above their phase transition temperatures and subjected to five freeze/thaw cycles with a vortex in between. Large unilamellar vesicles (LUVs) with a mean diameter of 0.1 μm were prepared from MLVs by the extrusion method[36] using polycarbonate filters (Nuclepore Corp., Cambridge, CA, USA). For FTIR spectroscopy, 200 μg of peptide was added to the appropriate amount of dried lipid and lyophilized. These samples were resuspended in 100 μL of D_2O buffer with 20 mM HEPES, 1 mM EDTA, and either 25 or 100 mM NaCl at pH 7.4, and MLVs were obtained as stated above. As a final step, samples were centrifuged at 14000 rpm at 25 °C for 10 min to eliminate unbound peptide. The pellet was resuspended in 25 μL of D_2O buffer and incubated for 45 min at 10 °C above the T_m of the lipid mixture. Both peptide and lipid concentration were measured by methods described elsewhere.[37,38]

Membrane Leakage Measurements. LUVs with a mean diameter of 0.1 μm were prepared as indicated above in buffer containing 10 mM Tris, 20 mM NaCl, pH 7.4 (at 25 °C), and 40 mM CF. Nonencapsulated CF was removed from the liposome suspension by using size-exclusion chromatography with Sephadex G-50 (GE Healthcare), with elution buffer composed of 10 mM Tris, 100 mM NaCl (except in the case of one single experiment with liver lipid extract where 40 mM NaCl was used), and 0.1 mM EDTA at pH 7.4. Membrane rupture (leakage) of intraliposomal CF was determined by exposing the CF-containing liposomes (final lipid concentration, 0.125 mM) with the appropriate amounts of peptide (peptide-to-lipid molar ratio of 1:25) on microtiter plates using a microplate reader (FLUOstar; BMG Labtech, Offenburg, Germany), stabilized at 25 °C, with each well containing 170 μL. Sample mixing was achieved by continuous shaking. Excitation and emission wavelengths were 492 and 517 nm, respectively. The maximum leakage value was defined as that achieved following the addition of Triton X-100 to attain a final concentration of 0.5% (w/w). Three fluorescence measurements were performed at different times: before the addition of the peptide, after its addition, and finally following Triton X-100 addition. The leakage induced by any of those peptides was defined according to the following equation, % Release = $100(F_f - F_0)/(F_{100} - F_0)$, where F_0 is the initial fluorescence of the vesicle suspension, F_f is the equilibrium value of fluorescence after peptide addition, and F_{100} is the fluorescence value after addition of Triton X-100. For further details, see refs 39 and 40.

Fluorescence Anisotropy of DPH in Membranes. MLVs were prepared as stated previously in buffer containing 20 mM HEPES either alone or containing different concentrations of NaCl or KCl at pH 7.4 and 25 °C. Aliquots of DPH in *N*,*N*′-dimethylformamide at 0.2 mM were added to the liposome preparation at a probe/lipid molar ratio of 1:500. DPH and its derivatives are widely used as probes to assess membrane dynamics and arrangement. DPH localizes into the hydrophobic core of the lipid palisade.[41] Preparations were incubated at 10 °C above the phase transition temperature T_m of the phospholipid mixture for 1 h. Subsequently, the peptides were added to obtain a peptide/lipid molar ratio of 1:15 and incubated for 1 h 10 °C above the T_m of each lipid, with occasional vortexing. Fluorescence experiments were carried out using 5 mm × 5 mm quartz cuvettes in a final volume of 400 μL (315 μM lipid concentration). The steady state fluorescence anisotropy was measured with an automated polarization accessory using a Varian Cary Eclipse fluorescence spectrometer, coupled to an automatized Peltier temperature changer. The vertically and horizontally polarized emission intensities were corrected for background scattering by subtracting the corresponding polarized intensities of a phospholipid preparation without DPH. The *G*-factor was determined by measuring the polarized components of the fluorescence of the probe with horizontally polarized excitation ($G = I_{HV}/I_{HH}$). Excitation and emission wavelengths were set as 360 and 430 nm, respectively, with 5 nm slits. Anisotropy values were calculated using the formula $\langle r \rangle = (I_{VV} - GI_{VH})/(I_{VV} + 2GI_{VH})$, where I_{VV} and I_{VH} are the measured fluorescence intensities with the excitation polarizer vertically oriented and the emission polarizer vertically and horizontally oriented, respectively.

Peptide Binding Using FPE-Labeled Membranes. LUVs with a mean diameter of 0.1 μM were obtained as stated previously and in a buffer containing 10 mM Tris−HCl at pH 7.4 (at 25 °C). As described elsewhere, only the outer bilayer leaflet was labeled with FPE.[42] LUVs were incubated with 0.1 mol % FPE dissolved in ethanol (never more than 0.1% of the total aqueous volume) at 37 °C for 1 h in the dark. Unincorporated FPE was removed by gel filtration on a Sephadex G-25 column equilibrated with the appropriate buffer. FPE vesicles were stored at 4 °C until use in an O_2-free atmosphere. The fluorescence of FPE-labeled vesicles was measured after the desired amount of peptide was directly added into 400 μL of lipid suspension (200 μM lipid) using a Varian Cary Eclipse fluorescence spectrometer. Excitation and emission wavelengths were 490 and 520 nm, respectively, with 5 nm slits. Temperature was maintained at 25 °C throughout the experiment. Background scattering was subtracted from probe free samples. Data were fitted to a hyperbolic binding model[43] considering the following formulas, $F = F_{max}[P]/(K_d + [P])$ or $F = F_{max}[P]^n/(K_d + [P]^n)$, where *F* is the fluorescence intensity, F_{max} the maximum fluorescence intensity, [P] the concentration of peptide, K_d the dissociation constant of the membrane binding process, and *n* the Hill coefficient.

Differential Scanning Calorimetry. MLVs were formed as stated above in 20 mM HEPES and different concentrations of NaCl at pH 7.4. Peptides were added to obtain a peptide/lipid molar ratio of 1:10 at a final lipid concentration of 600 μM. Samples were incubated 10 °C above the T_m of each lipid for 1 h with occasional vortexing. Before loading the samples into the calorimetric cell, samples were degassed under a vacuum for 10−15 min with gentle stirring. DSC experiments were performed in a VP-DSC differential scanning calorimeter (MicroCal LLC, MA) under a constant external pressure of 30 psi in order to avoid bubble formation. Samples were heated at a constant scan rate of 60 °C/h. Experimental data were corrected from small mismatches between the two cells by subtracting a buffer baseline prior to data analysis. The excess heat capacity functions were analyzed using Origin 7.0 (MicroCal software). The error in determination of T_c was 0.2 °C. The thermograms were defined by the onset and completion temperatures of the transition peaks obtained from heating scans. The phase transition temperature was defined as the temperature at the peak maximum. Only reproducible and reversible scans were considered for analysis.

Infrared Spectroscopy. A sample volume of 25 μL prepared as stated above was placed between CaF_2 windows separated by 50 μm thick Teflon spacers in a liquid demountable cell (Harrick, Ossining, NY). The spectra were obtained in a Bruker IF66S spectrometer using a DTGS

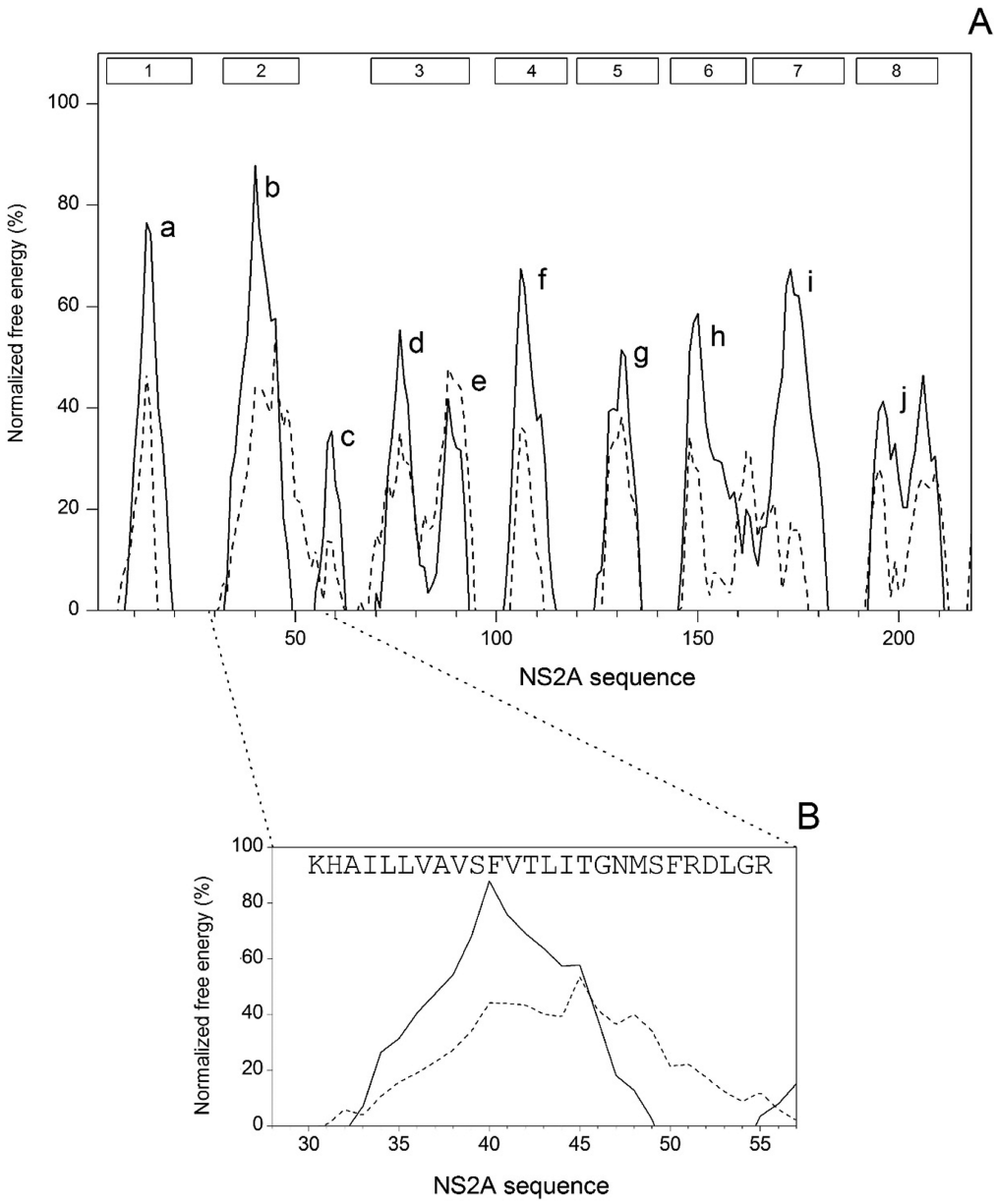

Figure 1. (A) Averaged normalized water-to-membrane (solid line) and water-to-interface (dashed line) transfer free energy scales applied to 41 DENV NS2A primary sequences. The NS2A sequences pertained to *DENV1* (02_20, 05K4147DK1, 297arg00, BIDV1323, BIDV1800, BIDV1841, BIDV1926VN2008, BIDV2143, BIDV2243VE2007 and ThD1004901), *DENV2* (NGC, BIDV633, BIDV687, CSF381, CSF63, DakArD20761, DF707, DF755, MD1504, MD903, and MD917), *DENV3* (05K797DK1, 07CHLS001, 98, 98TWmosq, BIDV1831VN2007, BIDV1874VN2007, BR29002, C036094, TB55i, and ThD31283_98), and *DENV4* (2A, BIDV2165VE1998, BIDV2170VE1999, H241, rDEN4del30, Sin897695, ThD4047697, ThD4048501, Vp4, and Yama) strains.[24,53] Transfer free energies (kcal/mol) were obtained from Wimley and White,[54] Engelman et al.,[55] Hessa et al.,[56] Moon and Fleming,[57] Meiler et al.,[58] and Eisenberg et al.[59] Regions 1−8[23] and a−j (this work) are depicted. (B) Enlargement of the 30−55 segment, showing the sequence of the dens25 peptide.

detector. Each spectrum was obtained by collecting 300 interferograms with a nominal resolution of 2 cm^{-1}. A fast Fourier transform algorithm with triangular apodization was applied, and a shuttle accessory was used to average both sample and background spectra in the same time frame. The spectrometer was continuously purged with dry air at a dew point of −40 °C. Samples were equilibrated at the lowest temperature for 20 min prior to acquisition. An external bath circulator, connected to the infrared spectrometer, controlled the sample temperature. For temperature studies, samples were scanned using 2 °C intervals and a 2 min delay. Data analysis methodologies were performed interactively using either GRAMS/32 or Spectra-Calc (Galactic Industriesm Salem, MA) as described elsewhere.[39,44]

RESULTS

NS2A is a membrane protein with possibly five transmembrane domains and at least two membrane interacting regions.[23] NS2A, essential in the viral RNA replication, is under-characterized possibly owing to its significant hydrophobicity. Therefore, a multitude of problems arise when trying to define structure, function, and lipid−protein interacting regions. We have conducted a screening of membrane-active regions of DENV NS2A protein, relying on a peptide library that

dx.doi.org/10.1021/jp504911r | J. Phys. Chem. B 2014, 118, 10142−10155

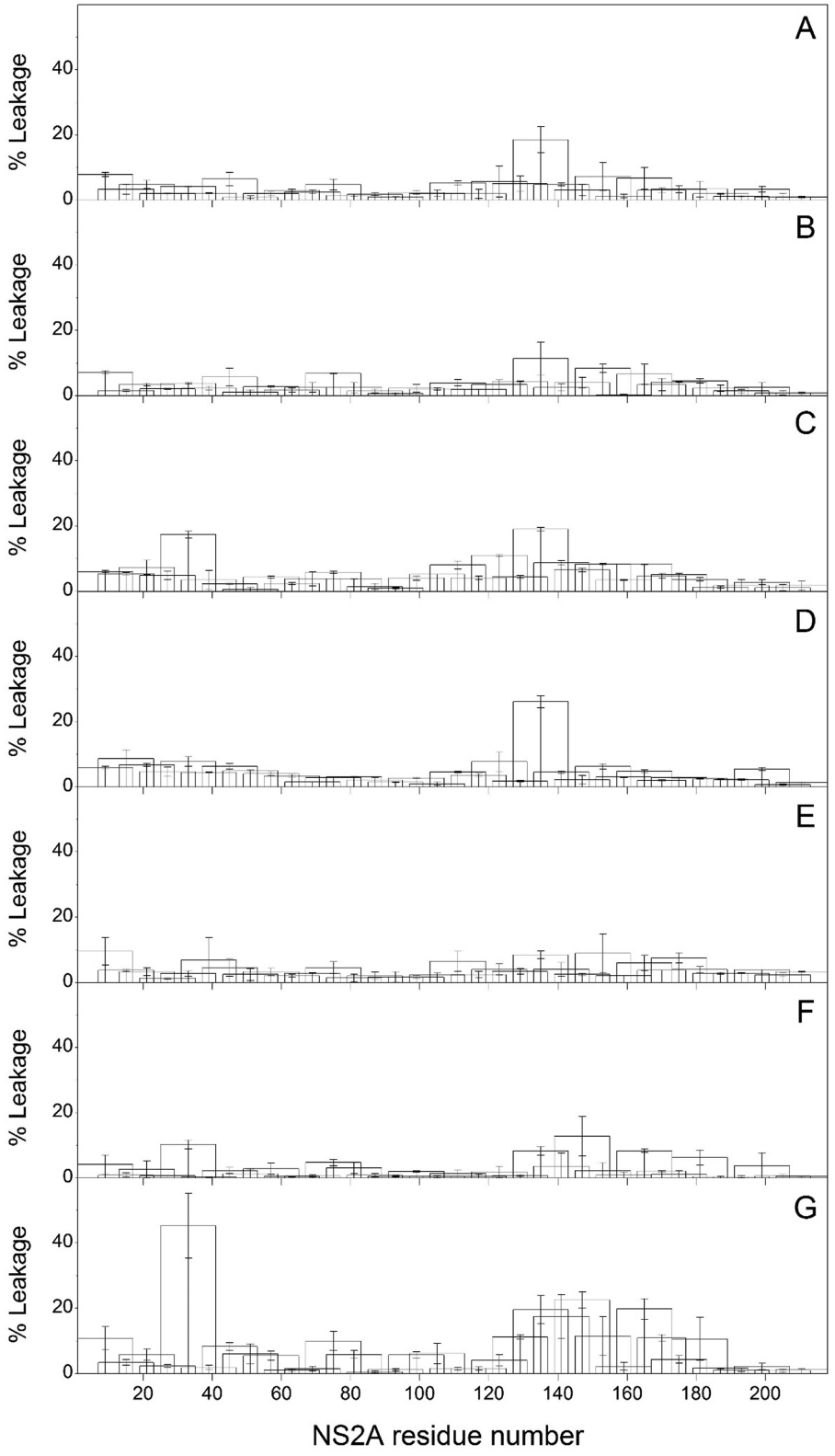

Figure 2. Membrane rupture (CF leakage) induced by the peptide library derived from DENV2 NS2A protein on LUVs composed of (A) EPC, (B) EPC/Chol at a molar proportion of 5:1, (C) EPC/BMP at a molar proportion of 5:1, (D) EPC/BPI at a molar proportion of 5:1, (E) EPC/ESM/Chol at a molar proportion of 5:2:1, (F) ER complex synthetic lipid mixture, and (G) liver lipid extract. Vertical bars represent standard deviations of the average of four samples.

represents the full length NS2A protein composed of 35 different overlapping peptides (Table 1). Because the library includes the complete linear sequence of this protein and each individual peptide, *i*, overlaps with two and three consecutive peptides, $i + 1$ and $i + 2$, by approximately 11 and 5 residues, respectively, the obtained data should be analyzed considering the effect of protein segments rather than that of isolated peptides. Furthermore, we have performed a thorough

dx.doi.org/10.1021/jp504911r | J. Phys. Chem. B 2014, 118, 10142−10155

characterization of the effect that a peptide coincident with a membrane-active region of protein NS2A, peptide dens25, has on different membrane model systems with interesting results, possibly important to highlight new therapeutic targets for DENV infection.

Assuming the 3D organization of NS2A's amino acids as an α-helix and applying it to the whole sequence,[31] the respective average normalized water-to-membrane and water-to-interface transfer free energy scales for each of the residues and for 35 DENV NS2A strain specific sequences have been obtained (Figure 1A). Ten distinct regions having considerable hydrophobic and interfacial values throughout the protein sequence can be resolved: region a encompassing residues from 6 to 19, region b from 30 to 54, region c from 55 to 62, region d from 70 to 83, region e from 83 to 93, region f from 101 to 115, region g from 124 to 136, region h from 145 to 164, region i from 165 to 182, and region j from 192 to 211. Xie et al.[23] suggested the existence of eight different regions for the NS2B topology: regions 1 (residues 3−24), 2 (residues 32−51), and 5 (residues 120−140) as peripheral segments and regions 3 (residues 69−93), 4 (residues 100−118), 6 (residues 143−163), 7 (residues 165−186), and 8 (residues 189−209) as transmembrane segments (see Figure 1A). Interestingly, regions a, b, and g coincide with regions 1, 2, and 5, whereas regions d−e, f, h, i, and j coincide with regions 3, 4, 6, 7, and 8. Region c has both a lower intensity and a smaller length than expected to be considered as either a membrane interacting domain or a transmembrane segment.[31] The existence of pre-transmembrane domains with a strong propensity for partitioning into membrane interfaces in different viral proteins is well-known.[31] These domains show characteristic high water-to-interface transfer free energies overlapping with high water-to-bilayer transfer free energies. Figure 1B shows the normalized water-to-bilayer and water-to-interface transfer free energies for NS2A region b encompassing amino acids 30−55 (the sequence is also shown). As observed, this segment has a significant high water-to-bilayer transfer free energy immediately followed by a region of high water-to-interface transfer free energy, a characteristic pattern of pre-transmembrane domains (so-called stem or membrane-proximal domains). This pattern is characterized by a strong propensity to partition into and interact with membrane interfaces,[25,45−52] suggesting that this segment might interact significantly with membranes. Region 2 is coincidental with region b, and has already been proposed to associate with the membrane.[23] It should not be ruled out that this domain's effect on membranes could be similar to other viral pre-transmembrane domains (see below).

The membrane leakage results for the NS2A peptide library are shown in Figure 2. We have considered seven different lipid compositions, simple and complex: EPC (Figure 2A), EPC/Chol at a phospholipid molar ratio of 5:1 (Figure 2B), EPC/BMP at a phospholipid molar ratio of 5:1 (Figure 2C), EPC/BPI at a phospholipid molar ratio of 5:1 (Figure 2D), and EPC/SM/Chol at a phospholipid molar ratio of 5:2:1 (Figure 2E), whereas the complex ones consisted of an ER synthetic lipid mixture resembling the ER membrane (Figure 2F) and a lipid extract of liver membranes (Figure 2G). The leakage data showed that some peptides exerted a quite significant leakage effect with a minor dependence on lipid composition. The leakage effects were focused on two segments, one segment delimited by residues 25−41 corresponding to peptide 5 and a long segment delimited by residues 103−183 (peptides 18−29). Leakage elicited by peptide 5 was remarkable in the presence of liver liposomes, since a leakage value of about 45% was observed (Figure 2G). Lower but significant values were found for liposomes containing BMP (about 18%, Figure 2C) and ER-like membranes (about 10%, Figure 2F). Leakage values elicited by peptides 18−29 were lower than that observed with peptide 5, oscillating between 10 and 20%. Apart from these differences, leakage induction was consistent throughout all liposome compositions used (Figure 2). Interestingly, peptide 5 overlaps region b and peptides 18−29 overlap regions f, g, h, and i. Peptide 5 would be defined by a significant leakage value concurrent with high hydrophobicity and interfaciality (see above) and therefore would partition extensively to the membrane interface.[31]

Phospholipids can undergo a cooperative melting reaction related to the increase in disorder of the lipid palisade; this melting process can be influenced by many types of molecules including peptides and proteins. To assess the influence of the NS2A peptide library on the structural and thermotropic properties of phospholipid membranes, we measured the temperature dependence of the steady-state fluorescence anisotropy of the fluorescent probe DPH incorporated into model biomembranes (DMPC, Supplemental Figure 1 (Supporting Information), and DMPG, Supplemental Figure 2 (Supporting Information)). There were no significant changes in the T_m values of DMPC in the presence of the NS2A derived peptides, but some of them, namely, peptides 2, 5, and 12, elicited a significant effect on anisotropy and cooperativity (Supplemental Figure 1, Supporting Information). In the case of DMPG, there were more peptides affecting the thermotropic behavior of the phospholipid (Supplemental Figure 2, Supporting Information). However, peptides 2, 5, 10, and 12 were the ones that showed a significant effect on the cooperativity, T_m, and/or the anisotropy of DMPG. These data would suggest that these peptides should interact with membranes at a relative deep location, considering that DPH is known to locate inside the palisade structure of the membrane. The specific effect that these peptides have on DMPG does not seem to be exclusively electrostatic, since the net charges of peptides having a remarkable effect, i.e., peptides 2, 5, 10, and 12, are −2, +2, −1, and 0, respectively (Table 1).

As shown above, peptide 5 presents a distinctive pattern characteristic of a membrane-proximal domain (Figure 1B), elicits a significant leakage value (Figure 2), and affects the thermotropic behavior of DMPC (Supplemental Figure 1, Supporting Information) and DMPG (Supplemental Figure 2, Supporting Information). Furthermore, the region where peptide 5 resides has been proposed to bind to the membrane surface.[23] Therefore, we have carried out a thorough characterization of peptide dens25, corresponding to the NS2A segment comprised by residues 30−55 and its membrane interactions in order to assess the membranotropic character of this protein region. Since peptide dens25 lacks a Trp residue and therefore intrinsic fluorescence, we considered the FPE probe,[40] sensitive to the electrostatic surface potential, to detect the binding extension of the peptide to membranes with distinct lipid compositions and lipid/peptide ratios (Figure 3A). Peptide dens25 showed a higher affinity for model membranes composed of negatively charged phospholipids, as well as the complex ER and liver lipid membranes. The dependence of peptide binding on the membrane surface total charge is demonstrated by the linear dependence of FPE fluorescence and EPG content for membranes containing different lipid

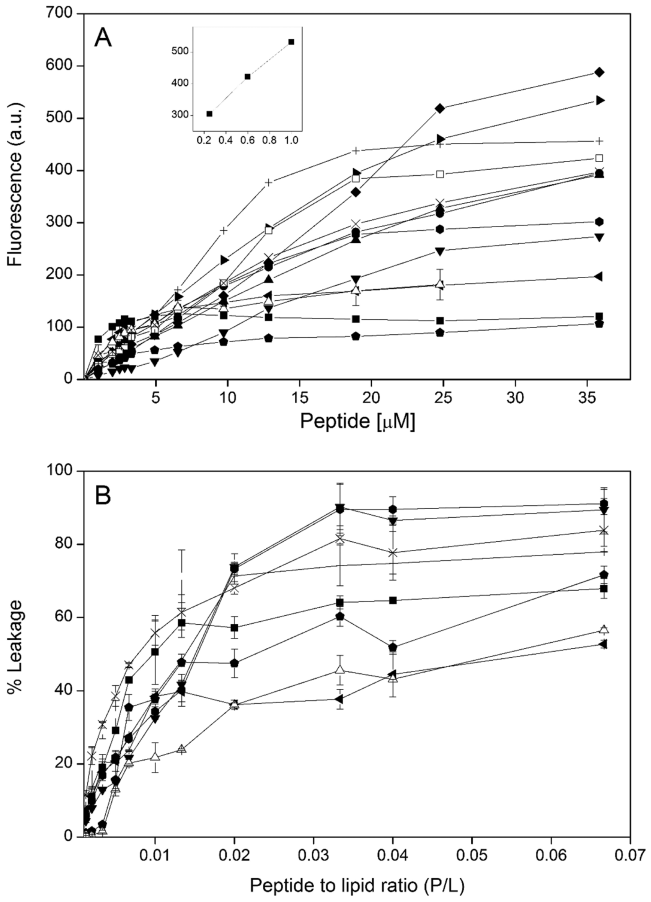

Figure 3. (A) Fluorescence signal amplitude of FPE versus dens25 peptide concentration to determine peptide binding to membrane model systems and (B) release (membrane rupture) of CF using different lipid compositions induced by dens25 peptide. The lipid compositions used were EPC (■), EPC/BPI at a molar proportion of 1:1 (●), EPC/CL at a molar proportion of 1:1 (▲), EPC/BPS at a molar proportion of 5:1 (▼), EPC/BPS at a molar proportion of 5:3 (◆), EPC/Chol at a molar proportion of 5:1 (◀), EPC/EPG at a molar proportion of 1:1 (▶), EPC/EPG at a molar proportion of 5:1 (⬢), EPC/EPG at a molar proportion of 5:3 (□), EPC/ESM at a molar proportion of 5:1 (⬟), EPC/ESM/Chol at a molar proportion of 5:1:1 (△), ER complex synthetic lipid mixture (+), and liver lipid extract (×). The buffer contained no NaCl in part A but 100 mM NaCl in part B. The inset shows the dependence of FPE fluorescence on EPC/EPG ratio for liposome compositions containing EPC and EPG and 36 μM peptide. See text for details.

molar ratios of EPC and EPG (Figure 3A, inset). A similar linear relationship is observed for EPC/BPS membranes (not shown). Interestingly, a lower affinity was observed for zwitterionic liposomes, i.e., those composed of EPC, EPC/Chol, and EPC/SM/Chol (Figure 3A). All FPE binding data could be adjusted to either a sigmoidal (Hill coefficient of approximately 1) or a hyperbolic binding model, suggesting that the peptide might interact with membranes as a monomer.

Peptide dens25 was able to induce the release of encapsulated CF in a dose- and composition-dependent manner (Figure 3B). Liposomes composed of EPC/EPG and EPC/BPS presented respective leakage values of 91 and 90% at peptide/lipid ratios of 0.066. Noteworthy leakage values were observed for liposomes composed of the ER-like complex mixture and the liver lipid extract, since, at the same peptide/lipid ratios, leakage values of 84 and 78% were found. Liposomes composed of EPC and EPC/ESM at a molar ratio of 5:1 presented similar leakage values of 68 and 71%, respectively. However, addition of Chol to these last lipid compositions, i.e., EPC/Chol at a molar ratio of 5:1 and EPC/ESM/Chol at a molar ratio of 5:1:1, significantly reduced the leakage values to 53 and 56%, respectively. From all of these data, it could be concluded that peptide dens25 exerts a higher leakage on liposomes composed of negatively charged phospholipids but a lower one when Chol is present.

As noted above, peptide dens25 seems to interact more significantly with negatively charged phospholipids, with this interaction being either with the phospholipid headgroup or with the negative charge or both. In order to discriminate between these possibilities, we have studied the contribution of ionic strength to the thermotropic phase behavior of the negatively charged phospholipid DMPG in the absence and in the presence of peptide dens25 by steady-state fluorescence anisotropy of the fluorescent probe DPH (Figure 4). In the absence of salts, the transition of pure DMPG was a broad one (Figure 4A), as it has been noted before.[60] In the presence of peptide dens25 at a lipid/peptide molar ratio of 10:1, the anisotropy of DMPG increased significantly above T_m (Figure 4A), but the cooperativity of the transition was similar to that found in pure DMPG (Figure 4M). When increasing concentrations of either NaCl (Figure 4C, E, G, I, and K) or KCl (Figure 4D, F, H, J, and L) were added to pure DMPG, the cooperativity of the phospholipid increased. However, when dens25 was present, the cooperativity of DMPG increased steadily, although slightly, at increasing concentrations of either NaCl or KCl (Figure 4M). As observed in the figure, even at a concentration of 300 mM of either NaCl or KCl, the cooperativity was lower than that found for the pure phospholipid but higher than the cooperativity found at lower salt concentrations. These data would suggest that the interaction between the peptide and the negatively charged phospholipids would be mainly of an electrostatic nature. The difference of anisotropy in the absence and in the presence of peptide is shown in Figure 4N. It can be observed that the difference is inversely proportional to the salt concentration, being lower for NaCl than for KCl, which would indicate that not only an increase in ionic strength reduces dens25's effect on membranes but also there are subtle differences between the sodium and potassium ions.

The effect of peptide dens25 on the thermotropic phase behavior of different phospholipids was studied using DSC (Figure 5). When properly hydrated and in the presence of salt, DMPC and DMPG display two endothermic peaks on heating, corresponding to the pretransition (appearing at about 12−14 °C, $L_{\beta'}-P_{\beta'}$) and the main transition (appearing at about 23−24 °C, $P_{\beta'}-L_{\alpha}$). Incorporation of dens25 into DMPC at a lipid/peptide ratio of 10:1 elicited no noticeable effect on the thermotropic behavior of the pure phospholipid, neither at low nor at high ionic strength (Figure 5A and B, respectively). In contrast, the main transition of pure DMPG at 25 mM NaCl was apparently composed of two different peaks, which should be due to mixed phases (Figure 5C). Incorporation of peptide dens25 induced a significant lowering of the cooperativity of the transition, but no apparent changes to the number of peaks were clearly visible (Figure 5C). In the presence of 100 mM NaCl, the main transition of pure DMPG was composed of only one peak, as expected, showing a large cooperativity (Figure 5D). When dens25 was incorporated into the membrane, a broad main transition peak was observed,

dx.doi.org/10.1021/jp504911r | J. Phys. Chem. B 2014, 118, 10142−10155

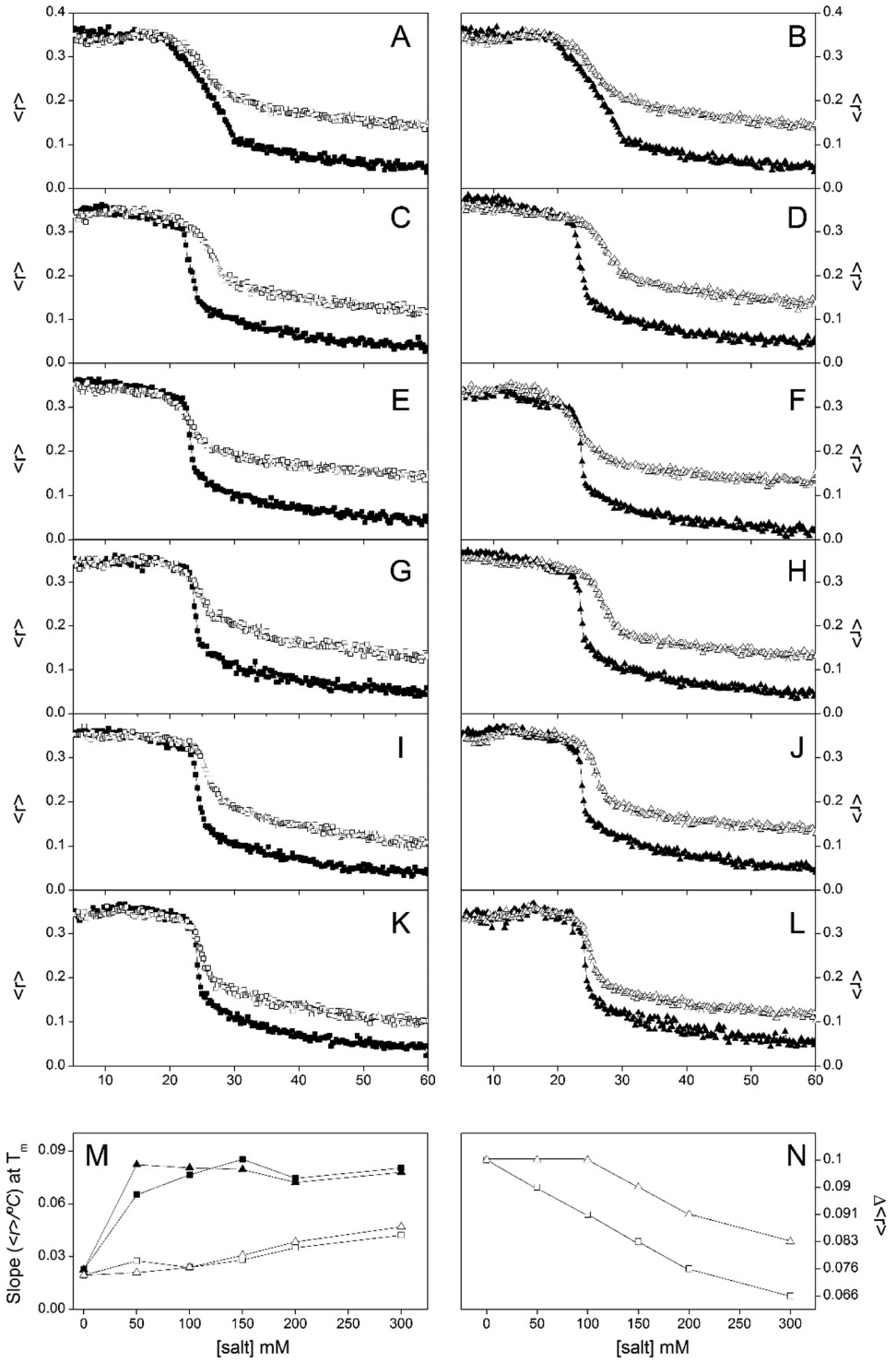

Figure 4. Temperature dependence of the steady-state anisotropy $\langle r \rangle$ of the DPH probe incorporated into DMPG membranes at pH 7.4 in the absence (■, ▲) and in the presence (□, △) of peptide dens25 at a peptide/lipid molar ratio of 1:10 and in the presence of different concentrations of NaCl (■, □) or KCl (▲, △). Buffers contained 20 mM HEPES, 0.1 mM EDTA, and (A) 0 mM NaCl, (B) 0 mM KCl, (C) 50 mM NaCl, (D) 50 mM KCl, (E) 100 mM NaCl, (F) 100 mM KCl, (G) 150 mM NaCl, (H) 150 mM KCl, (I) 200 mM Na Cl, (J) 200 mM KCl, (K) 300 mM NaCl, and (L) 300 mM KCl. The value of the first derivative of $\langle r \rangle$ with respect to temperature for each sample at its absolute minimum ($T = T_m$) is shown in part M, whereas the difference in $\langle r \rangle$ at 40 °C between the pure lipid and lipid plus is shown in part N.

indicating a significant lowering in cooperativity (Figure 5D). The pattern observed at 300 mM NaCl for pure DMPG was similar to the one found at 100 mM NaCl, since only one very cooperative peak was observed (Figure 5E and D, respectively). The addition of peptide dens25 lowered the cooperativity of the main transition, but the width at 300 mM NaCl was narrower than that at 100 mM, indicating that an increase of NaCl concentration induced an increase in the cooperativity of its transition (Figure 5D and E). In the case of DMPS, a similar pattern was visible. In the presence of 25 mM NaCl, peptide

dx.doi.org/10.1021/jp504911r | J. Phys. Chem. B 2014, 118, 10142−10155

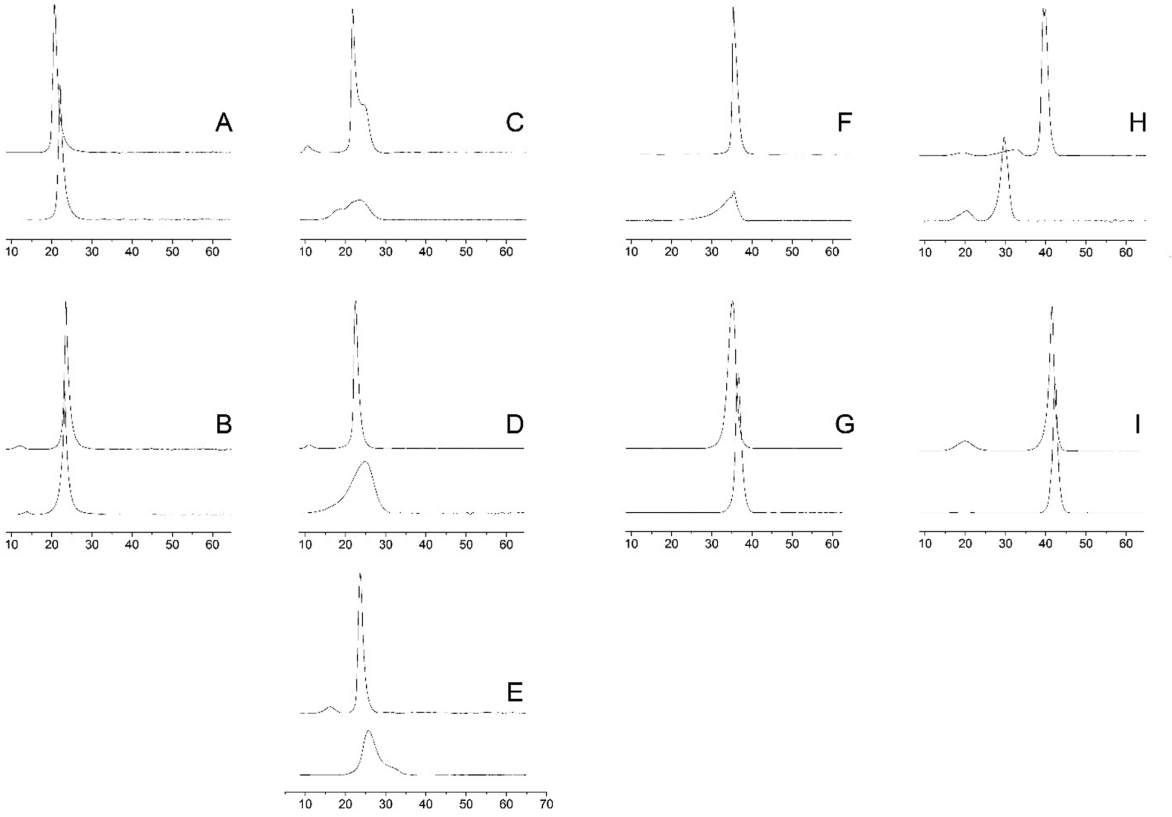

Figure 5. Differential scanning calorimetry heating thermograms corresponding to model membranes of DMPC (A and B), DMPG (C, D, and E), DMPS (F and G), and BMP (H and I) in the absence (top curves) and in the presence of peptide dens25 (bottom curves) at a phospholipid/peptide molar ratio of 10:1. The buffer contained 20 mM HEPES, 0.1 mM EDTA, pH 7.4, and one of the following NaCl concentrations: 25 mM NaCl (A, C, F, and H), 100 mM NaCl (B, D, G, and I), or 300 mM NaCl (E). All thermograms were normalized according to lipid concentration.

dens25 induced a significant decrease in cooperativity in DMPS if compared to the pure lipid sample (Figure 5F), whereas in the presence of 100 mM NaCl the peptide barely affected the main transition of the phospholipid (Figure 5G). In the presence of 25 mM NaCl, 14BMP, a negatively charged phospholipid, presented two low-enthalpy peaks and one high-enthalpy peak (Figure 5H). In the presence of dens25, two peaks were observed, a low-enthalpy peak and a high-enthalpy one, the latter displaced to lower temperatures when compared to the pure lipid. In the presence of 100 mM NaCl, 14BMP presented a normal pattern, i.e., a low-enthalpy peak and a high-enthalpy peak corresponding to the $L_{c1}-L_{c2}$ and $L_{c2}-L_{\alpha}$ transitions (Figure 5I). Apart from abolishing the low-enthalpy peak, peptide dens25 did not exert any other significant effect on the high-enthalpy high-temperature peak (Figure 5I). These DSC data would suggest that peptide dens25 affects more significantly the phase transition of negatively charged phospholipids in the absence of salt, an effect that is significantly increased when the ionic strength is reduced; i.e., the less salt concentration, the bigger the effect dens25 has on negatively charged phospholipids.

To further explore the effects of peptide dens25 on different types of model membranes, we have studied the ester C═O stretching band of DMPC and DMPG, which appears between 1745 and 1720 cm^{-1} in infrared spectroscopy (Figure 6). The frequency maximum of the ester C═O band of pure DMPC in the presence of 25 mM NaCl had two transitions, one at about 17 °C and the other at about 23 °C, coincident with the pretransition and main gel to liquid crystalline phase transition of the pure phospholipid (Figure 6A). When dens25 was present, the frequency of the ester C═O band of DMPC displayed only one transition at about 24 °C (Figure 6A). Nonetheless, its frequency maximum was higher in the presence of the peptide than in its absence, suggesting that the peptide increased the intensity of the 1743 cm^{-1} component relative to the 1727 cm^{-1} one; i.e., the quantity of non-hydrogen-bonded C═O ester bands increased in the presence of dens25.[61,62] In the presence of 100 mM NaCl, a relatively similar pattern was found for DMPC (Figure 6B). The frequency maximum of the ester C═O band of the pure phospholipid displayed two transitions at about 16 and 24 °C, i.e., the pretransition and the main phase transition (Figure 6A). In the presence of the peptide, the frequency of the ester C═O band displayed two transitions, a broad one at about 16 °C and a narrow one at 24 °C. As before, its absolute frequency was higher in the presence of dens25 than in its absence; however, it was not as high as it was found in the presence of 25 mM NaCl (compare parts A and B of Figure 6). The frequency maximum of the ester C═O band of pure DMPG in the presence of 25 mM NaCl displayed two transitions, a broad one at about 14 °C and a narrow one at 23 °C, coincident with the pretransition and main phase transition of the pure phospholipid in accordance with the DSC data (Figure 6C). Noteworthy is the result that the frequency of the ester C═O band of DMPG in the presence of dens25 displayed no transition at all in the temperature range studied (Figure 6C). In the presence of 100 mM NaCl, the frequency maximum of the ester C═O band of pure DMPG displayed two transitions, a broad one at about 14 °C and a relatively cooperative one at 22 °C, coincident with the pre- and main transition of the pure

dx.doi.org/10.1021/jp504911r | J. Phys. Chem. B 2014, 118, 10142−10155

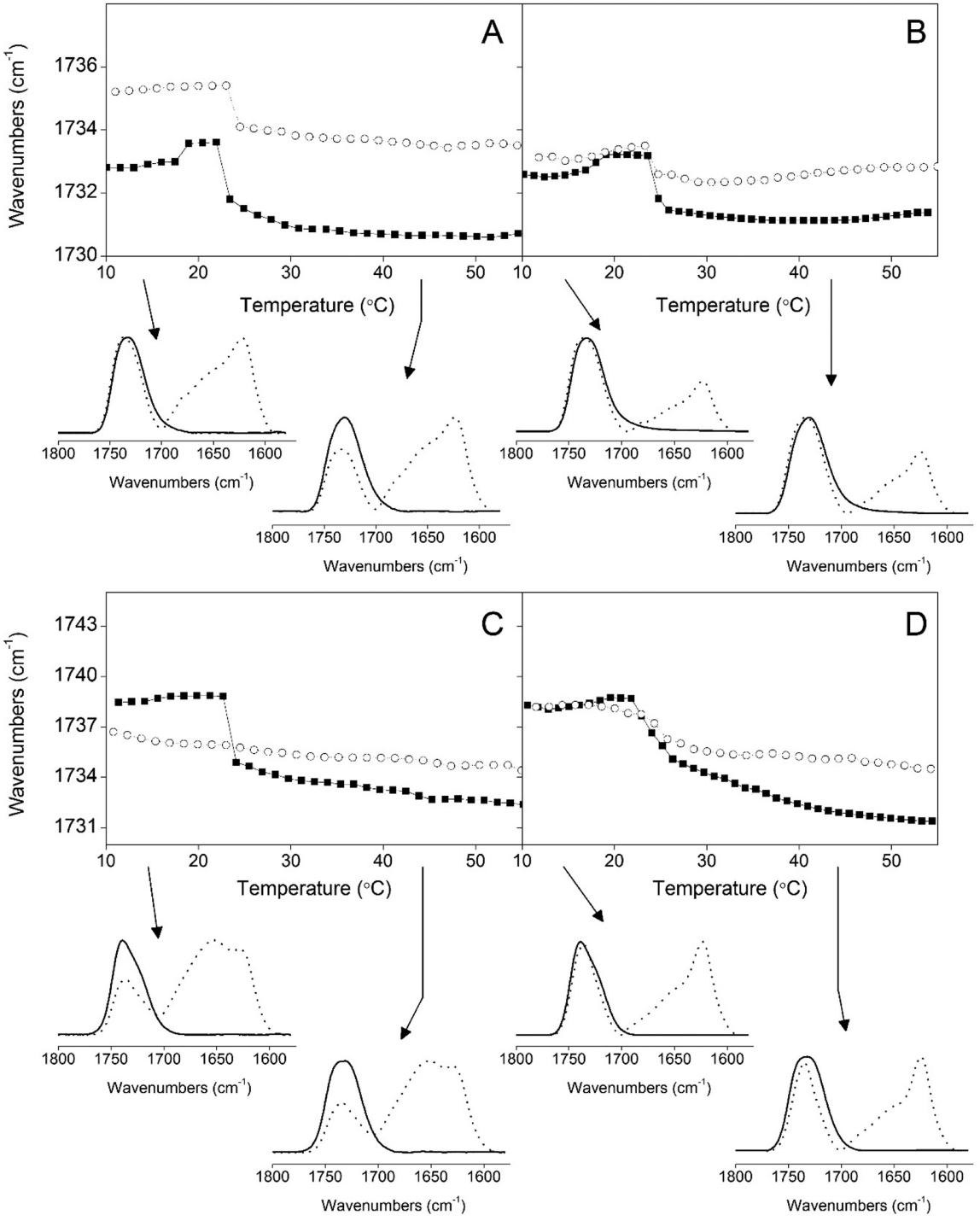

Figure 6. Temperature dependence of the frequencies of the C═O carbonyl stretching band of DMPC (A and B) and DMPG (C and D) in the absence (■) and in the presence (○) of peptide dens25. The buffer contained 20 mM HEPES, 0.1 mM EDTA, and either 25 mM NaCl (A, C) or 100 mM NaCl (B, D) at pH 7.4. Representative spectra of the membrane model systems in the absence (solid line) and in the presence (dashed line) of peptide dens25 are also shown. The phospholipid/peptide molar ratio was 15:1.

phospholipid (Figure 6C). In the presence of the dens25 peptide, the frequency of the ester C═O band displayed only a broad transition at about 24 °C, in accordance with the calorimetric data (Figure 6D). Its absolute frequency was higher in the presence of the peptide than in its absence but at temperatures higher than the main transition (Figure 6D). All these data would suggest that dens25 affects the phase transition of DMPG, a negatively charged phospholipid, but not that of DMPC, a zwitterionic one, in the presence of relatively low concentrations of NaCl. Conversely, the interaction of peptide dens25 with DMPG is abolished at relatively high salt concentrations.

We have also studied the overall secondary structure of dens25 in the presence of DMPC and DMPG at different salt concentrations by analyzing the dens25 infrared amide I′ band (Figure 6). The infrared amide I′ spectra of fully hydrated dens25 in the presence of DMPC and 25 mM NaCl below and above the lipid's main phase transition temperature are shown

dx.doi.org/10.1021/jp504911r | J. Phys. Chem. B 2014, 118, 10142−10155

in Figure 6A. At both temperatures, the amide I′ band presented two bands appearing at about 1623 and 1648 cm^{-1}, the former with relative lower intensity than the latter. The bands at about 1623 and 1648 cm^{-1} arise from the presence of aggregated β structures and mainly unordered and helical structures, respectively.[63,64] Upon data fitting, the relative intensity of the 1648 cm^{-1} band was about 73% and about 27% for the 1623 cm^{-1} band. In the presence of 100 mM NaCl and below and above the main transition of the phospholipid, the amide I′ band of dens25 presented a similar pattern, i.e., two bands at about 1648 and 1623 cm^{-1}, with relative intensities of 68 and 32%, respectively (Figure 6B). The infrared amide I′ spectra of fully hydrated dens25 in the presence of DMPG and 25 mM NaCl below and above the main phase transition of the phospholipid are shown in Figure 6C. In this case and in contrast to the DMPC sample, the amide I′ band of dens25 presented two bands with slightly different frequencies. These two bands have a maximum at about 1653 and 1626 cm^{-1}, and their relative intensities were about 85 and about 15%, respectively (Figure 6C). When 100 mM NaCl, both below and above the main transition of the phospholipid, the amide I′ band of dens25 presented two bands, but their frequencies were slightly different than in the presence of 25 mM NaCl, about 1648 and 1622 cm^{-1} (Figure 6D). In this case, the relative intensities of these two bands were also different, since it was found that they were 68 and 32%, respectively. From this picture, it is quite obvious that, in the presence of DMPG and at low NaCl concentration, the secondary structure of dens25 is different from that at high NaCl concentration, and this one presents a similar pattern to that found in the presence of DMPC at both low and high salt concentration. Although aggregated structures and helical and disordered structures are present in all samples, the quantity of aggregated β structures diminished dramatically; i.e., the relative amount of either helical or disordered or both increased in the presence of DMPG, a negatively charged phospholipid, and a low salt concentration.

DISCUSSION

DENV NS2A protein is essential in the viral replication process, yet it is a poorly characterized highly hydrophobic protein and requires the membrane to perform its functions. In this work, we have characterized its membrane active regions by using a NS2A derived peptide library and have identified several regions with different interacting capabilities. Additionally, we have characterized a NS2A peptide, peptide dens25, with interesting properties in the presence of membrane model systems with different compositions. We conducted a thorough biophysical study to ascertain the membrane disrupting capability of this region by studying the structural and dynamic features which might be relevant for those interactions.

We have been able to distinguish 10 different regions with significant hydrophobicity and interfacial values in NS2A. One of these regions, region b, showed increased and overlapping water-to-interface and water-to-bilayer transfer free energies. We have also studied the effect of a NS2A peptide library on membrane leakage and two segments with significant rupture capabilities were delineated, one segment delimited by residues 25−41 corresponding to peptide 5 and a long segment delimited by residues 103−183 corresponding to peptides 18−29. Interestingly, peptide 5 overlapped with region b and peptides 18−29 encompass a broad region where the supposed transmembrane segments of NS2A reside. We also studied the influence of the NS2A derived peptide library on the thermotropic properties of phospholipid membranes and found several peptides (peptides 2, 5, 10, and 12) which induced a noticeable effect on the cooperativity and the anisotropy of the phospholipids studied. Since peptide 5 presents a distinctive pattern, elicits a significant leakage value, affects the thermotropic behavior of both DMPC and DMPG, and has been proposed to bind to the membrane surface,[23] we have selected the NS2A segment comprised by residues 30−55, peptide dens25, to characterize its effect on model membranes.

Peptide dens25 bound extensively to model membranes composed of negatively charged phospholipids, and its binding was apparently dependent on membrane surface total charge, i.e., the more negative, the greater the binding. The dens25 peptide affected membrane stability, resulting in the release of CF, this effect being dependent on the lipid/peptide molar ratio and lipid composition. Interestingly, the highest CF release was observed for liposomes containing negatively charged phospholipids, whereas Chol induced lower leakage values. We have also shown that dens25 affected the steady state fluorescence anisotropy of DPH inserted into membranes, especially when those membranes were composed of negatively charged phospholipids. Significantly, the interaction of dens25 seemed to be of an electrostatic nature: the data indicated that the effect was inversely proportional to the salt concentration in the medium. Calorimetric experiments further corroborated these results, with peptide dens25 affecting more significantly the phase transition of membranes containing negatively charged phospholipids in the absence of salt, an effect that was significantly reduced when the ionic strength was increased; i.e., the less salt concentration, the bigger the effect dens25 has on negatively charged phospholipids. These results were also corroborated by the infrared analysis of the ester C═O stretching carbonyl band of the lipids. In the presence of low salt concentrations, dens25 affected the phase transition of the negatively charged molecule, DMPG, but not the zwitterionic one, DMPC. This interaction was abolished when the peptide was in the presence of increased salt concentrations.

In the infrared spectra of the amide I′ region of the fully hydrated dens25 peptide in the presence of different phospholipids and at different temperatures, coexistence of unordered, aggregated, and helical structures was clearly seen. However, the relative proportion of secondary structures varied depending on phospholipid type and salt concentration. In the presence of DMPG and at low NaCl concentration, the secondary structure of dens25 was different from that at high NaCl concentration, and this one was similar to that found in the presence of DMPC at both low and high salt concentration. Although aggregated structures and helical and disordered structures were present in all samples, the quantity of aggregated β structures diminished dramatically; i.e., the relative amount of either helical or disordered or both increased if negative lipids were present and the salt concentration was kept at low levels. The secondary structure of the dens25 peptide was thus affected by its binding to the membrane, as it has been suggested for other peptides.[53,65] Concomitantly, differences in the frequency of the carbonyl band of the phospholipids were observed, showing that peptide binding modulates phospholipid conformation.

Taking all of these results together, it is clear that this NS2A segment interacts electrostatically with the membrane when negatively charged phospholipids are present. The effect elicited by peptide dens25 should be primarily due to the

electrostatic nature of the phospholipids, i.e., charge, with a slight contribution of hydrophobic interactions. Interestingly, peptide dens25 affects membranes at distinct levels, from the membrane surface down to the hydrophobic core. Its location should be at or near the membrane interface, affecting lipid fluidity, most probably having an in-plane orientation. Moreover, its interfacial properties suggest that this region could behave similarly to a pre-transmembrane domain partitioning into and interacting with the membrane depending on the membrane composition and/or other proteins, shifting between membrane bound and unbound conformations and thus affecting its membrane topology.

CONCLUSIONS

The results described in this work highlight an interesting and important domain in the DENV NS2A protein which, due to its capacity to modulate and affect membrane structure, might be essential in the Dengue virus life cycle. Moreover, an understanding of NS2A and its interaction with the membrane during the DENV replication cycle might pave the way to pinpoint novel targets to address DENV infection.

ASSOCIATED CONTENT

Supporting Information

Two figures displaying the steady-state anisotropy of the DPH probe incorporated into DMPC and DMPG model membranes in the presence of the peptide library corresponding to DENV NS2A at pH 7.4. This material is available free of charge via the Internet at http://pubs.acs.org.

AUTHOR INFORMATION

Corresponding Author

*Phone: +34 966 658 762. Fax: +34 966 658 758. E-mail: jvillalain@umh.es.

Notes

The authors declare no competing financial interest.

ACKNOWLEDGMENTS

The research conducted in this work was partially funded by grant BFU2008-02617-BMC (Ministerio de Ciencia y Tecnología, Spain) to J.V. We owe a debt of gratitude to BEI Resources, National Institute of Allergy and Infectious Diseases, Manassas, VA, USA, for the peptides used in this work. H.N. has an FPU fellowship from MECD (Ministerio de Educación, Cultura y Deporte), Spain.

REFERENCES

(1) *Molecular Virology and Control of Flaviviruses*; Shi, P.-Y., Ed.; Caister Academic Press: Norfolk, U.K., 2012.

(2) Bhatt, S.; Gething, P. W.; Brady, O. J.; Messina, J. P.; Farlow, A. W.; Moyes, C. L.; Drake, J. M.; Brownstein, J. S.; Hoen, A. G.; Sankoh, O.; et al. The Global Distribution and Burden of Dengue. *Nature* **2013**, *496*, 504−507.

(3) WHO. *Dengue: Guidelines for Diagnosis, Treatment, Prevention and Control*; World Health Organization: Geneva, Switzerland: 2009.

(4) Pastorino, B.; Nougairede, A.; Wurtz, N.; Gould, E.; de Lamballerie, X. Role of Host Cell Factors in Flavivirus Infection: Implications for Pathogenesis and Development of Antiviral Drugs. *Antiviral Res.* **2010**, *87*, 281−294.

(5) Noble, C. G.; Chen, Y. L.; Dong, H.; Gu, F.; Lim, S. P.; Schul, W.; Wang, Q. Y.; Shi, P. Y. Strategies for Development of Dengue Virus Inhibitors. *Antiviral Res.* **2010**, *85*, 450−462.

(6) Perera, R.; Kuhn, R. J. Structural Proteomics of Dengue Virus. *Curr. Opin. Microbiol.* **2008**, *11*, 369−377.

(7) Bressanelli, S.; Stiasny, K.; Allison, S. L.; Stura, E. A.; Duquerroy, S.; Lescar, J.; Heinz, F. X.; Rey, F. A. Structure of a Flavivirus Envelope Glycoprotein in Its Low-Ph-Induced Membrane Fusion Conformation. *EMBO J.* **2004**, *23*, 728−738.

(8) Kielian, M.; Rey, F. A. Virus Membrane-Fusion Proteins: More Than One Way to Make a Hairpin. *Nat. Rev. Microbiol.* **2006**, *4*, 67−76.

(9) Mukhopadhyay, S.; Kuhn, R. J.; Rossmann, M. G. A Structural Perspective of the Flavivirus Life Cycle. *Nat. Rev. Microbiol.* **2005**, *3*, 13−22.

(10) Miller, S.; Kastner, S.; Krijnse-Locker, J.; Buhler, S.; Bartenschlager, R. The Non-Structural Protein 4a of Dengue Virus Is an Integral Membrane Protein Inducing Membrane Alterations in a 2k-Regulated Manner. *J. Biol. Chem.* **2007**, *282*, 8873−8882.

(11) Miller, S.; Krijnse-Locker, J. Modification of Intracellular Membrane Structures for Virus Replication. *Nat. Rev. Microbiol.* **2008**, *6*, 363−374.

(12) Welsch, S.; Miller, S.; Romero-Brey, I.; Merz, A.; Bleck, C. K.; Walther, P.; Fuller, S. D.; Antony, C.; Krijnse-Locker, J.; Bartenschlager, R. Composition and Three-Dimensional Architecture of the Dengue Virus Replication and Assembly Sites. *Cell Host Microbe* **2009**, *5*, 365−375.

(13) Brault, J. B.; Kudelko, M.; Vidalain, P. O.; Tangy, F.; Despres, P.; Pardigon, N. The Interaction of Flavivirus M Protein with Light Chain Tctex-1 of Human Dynein Plays a Role in Late Stages of Virus Replication. *Virology* **2011**, *417*, 369−378.

(14) Catteau, A.; Kalinina, O.; Wagner, M. C.; Deubel, V.; Courageot, M. P.; Despres, P. Dengue Virus M Protein Contains a Proapoptotic Sequence Referred to as Apoptom. *J. Gen. Virol.* **2003**, *84*, 2781−2793.

(15) Catteau, A.; Roue, G.; Yuste, V. J.; Susin, S. A.; Despres, P. Expression of Dengue Apoptom Sequence Results in Disruption of Mitochondrial Potential and Caspase Activation. *Biochimie* **2003**, *85*, 789−793.

(16) Mackenzie, J. M.; Khromykh, A. A.; Jones, M. K.; Westaway, E. G. Subcellular Localization and Some Biochemical Properties of the Flavivirus Kunjin Nonstructural Proteins Ns2a and Ns4a. *Virology* **1998**, *245*, 203−215.

(17) Miller, S.; Sparacio, S.; Bartenschlager, R. Subcellular Localization and Membrane Topology of the Dengue Virus Type 2 Non-Structural Protein 4b. *J. Biol. Chem.* **2006**, *281*, 8854−8863.

(18) Munoz-Jordan, J. L.; Sanchez-Burgos, G. G.; Laurent-Rolle, M.; Garcia-Sastre, A. Inhibition of Interferon Signaling by Dengue Virus. *Proc. Natl. Acad. Sci. U. S. A.* **2003**, *100*, 14333−14338.

(19) Rodenhuis-Zybert, I. A.; Wilschut, J.; Smit, J. M. Dengue Virus Life Cycle: Viral and Host Factors Modulating Infectivity. *Cell. Mol. Life Sci.* **2010**, *67*, 2773−2786.

(20) Muller, D. A.; Young, P. R. The Flavivirus Ns1 Protein: Molecular and Structural Biology, Immunology, Role in Pathogenesis and Application as a Diagnostic Biomarker. *Antiviral Res.* **2013**, *98*, 192−208.

(21) Falgout, B.; Chanock, R.; Lai, C. J. Proper Processing of Dengue Virus Nonstructural Glycoprotein Ns1 Requires the N-Terminal Hydrophobic Signal Sequence and the Downstream Nonstructural Protein Ns2a. *J. Virol.* **1989**, *63*, 1852−1860.

(22) Hori, H.; Lai, C. J. Cleavage of Dengue Virus Ns1-Ns2a Requires an Octapeptide Sequence at the C Terminus of Ns1. *J. Virol.* **1990**, *64*, 4573−4577.

(23) Yeagle, P. L.; Young, J.; Hui, S. W.; Epand, R. M. On the Mechanism of Inhibition of Viral and Vesicle Membrane Fusion by Carbobenzoxy-D-Phenylalanyl-L-Phenylalanylglycine. *Biochemistry* **1992**, *31*, 3177−3183.

(24) Guillen, J.; Perez-Berna, A. J.; Moreno, M. R.; Villalain, J. Identification of the Membrane-Active Regions of the Severe Acute Respiratory Syndrome Coronavirus Spike Membrane Glycoprotein Using a 16/18-Mer Peptide Scan: Implications for the Viral Fusion Mechanism. *J. Virol.* **2005**, *79*, 1743−1752.

(25) Moreno, M. R.; Giudici, M.; Villalain, J. The Membranotropic Regions of the Endo and Ecto Domains of Hiv Gp41 Envelope Glycoprotein. *Biochim. Biophys. Acta* **2006**, *1758*, 111−123.
(26) Nemesio, H.; Palomares-Jerez, F.; Villalain, J. The Membrane-Active Regions of the Dengue Virus Proteins C and E. *Biochim. Biophys. Acta* **2011**, *1808*, 2390−2402.
(27) Nemesio, H.; Palomares-Jerez, F.; Villalain, J. Ns4a and Ns4b Proteins from Dengue Virus: Membranotropic Regions. *Biochim. Biophys. Acta* **2012**, *1818*, 2818−2830.
(28) Perez-Berna, A. J.; Moreno, M. R.; Guillen, J.; Bernabeu, A.; Villalain, J. The Membrane-Active Regions of the Hepatitis C Virus E1 and E2 Envelope Glycoproteins. *Biochemistry* **2006**, *45*, 3755−3768.
(29) Perez-Berna, A. J.; Veiga, A. S.; Castanho, M. A.; Villalain, J. Hepatitis C Virus Core Protein Binding to Lipid Membranes: The Role of Domains 1 and 2. *J. Viral Hepatitis* **2008**, *15*, 346−356.
(30) Perez-Berna, A. J.; Guillen, J.; Moreno, M. R.; Bernabeu, A.; Pabst, G.; Laggner, P.; Villalain, J. Identification of the Membrane-Active Regions of Hepatitis C Virus P7 Protein: Biophysical Characterization of the Loop Region. *J. Biol. Chem.* **2008**, *283*, 8089−8101.
(31) Palomares-Jerez, F.; Nemesio, H.; Villalain, J. The Membrane Spanning Domains of Protein Ns4b from Hepatitis C Virus. *Biochim. Biophys. Acta* **2012**, *1818*, 2958−2966.
(32) Surewicz, W. K.; Mantsch, H. H.; Chapman, D. Determination of Protein Secondary Structure by Fourier Transform Infrared Spectroscopy: A Critical Assessment. *Biochemistry* **1993**, *32*, 389−394.
(33) Zhang, Y. P.; Lewis, R. N.; Hodges, R. S.; McElhaney, R. N. Ftir Spectroscopic Studies of the Conformation and Amide Hydrogen Exchange of a Peptide Model of the Hydrophobic Transmembrane Alpha-Helices of Membrane Proteins. *Biochemistry* **1992**, *31*, 11572−11578.
(34) Krainev, A. G.; Ferrington, D. A.; Williams, T. D.; Squier, T. C.; Bigelow, D. J. Adaptive Changes in Lipid Composition of Skeletal Sarcoplasmic Reticulum Membranes Associated with Aging. *Biochim. Biophys. Acta* **1995**, *1235*, 406−418.
(35) Keenan, T. W.; Morre, D. J. Phospholipid Class and Fatty Acid Composition of Golgi Apparatus Isolated from Rat Liver and Comparison with Other Cell Fractions. *Biochemistry* **1970**, *9*, 19−25.
(36) Mayer, L. D.; Hope, M. J.; Cullis, P. R. Vesicles of Variable Sizes Produced by a Rapid Extrusion Procedure. *Biochim. Biophys. Acta* **1986**, *858*, 161−168.
(37) Böttcher, C. S. F.; Van Gent, C. M.; Fries, C. A Rapid and Sensitive Sub-Micro Phosphorus Determination. *Anal. Chim. Acta* **1961**, *1061*, 203−204.
(38) Edelhoch, H. Spectroscopic Determination of Tryptophan and Tyrosine in Proteins. *Biochemistry* **1967**, *6*, 1948−1954.
(39) Bernabeu, A.; Guillen, J.; Perez-Berna, A. J.; Moreno, M. R.; Villalain, J. Structure of the C-Terminal Domain of the Pro-Apoptotic Protein Hrk and Its Interaction with Model Membranes. *Biochim. Biophys. Acta* **2007**, *1768*, 1659−1670.
(40) Moreno, M. R.; Guillen, J.; Perez-Berna, A. J.; Amoros, D.; Gomez, A. I.; Bernabeu, A.; Villalain, J. Characterization of the Interaction of Two Peptides from the N Terminus of the Nhr Domain of Hiv-1 Gp41 with Phospholipid Membranes. *Biochemistry* **2007**, *46*, 10572−10584.
(41) Lentz, B. R. Use of Fluorescent Probes to Monitor Molecular Order and Motions within Liposome Bilayers. *Chem. Phys. Lipids* **1993**, *64*, 99−116.
(42) Wall, J.; Ayoub, F.; O'Shea, P. Interactions of Macromolecules with the Mammalian Cell Surface. *J. Cell Sci.* **1995**, *108* (Pt 7), 2673−2682.
(43) Golding, C.; Senior, S.; Wilson, M. T.; O'Shea, P. Time Resolution of Binding and Membrane Insertion of a Mitochondrial Signal Peptide: Correlation with Structural Changes and Evidence for Cooperativity. *Biochemistry* **1996**, *35*, 10931−10937.
(44) Giudici, M.; Poveda, J. A.; Molina, M. L.; de la Canal, L.; Gonzalez-Ros, J. M.; Pfuller, K.; Pfuller, U.; Villalain, J. Antifungal Effects and Mechanism of Action of Viscotoxin A3. *FEBS J.* **2006**, *273*, 72−83.
(45) Guillen, J.; Perez-Berna, A. J.; Moreno, M. R.; Villalain, J. A Second Sars-Cov S2 Glycoprotein Internal Membrane-Active Peptide. Biophysical Characterization and Membrane Interaction. *Biochemistry* **2008**, *47*, 8214−8224.
(46) Shnaper, S.; Sackett, K.; Gallo, S. A.; Blumenthal, R.; Shai, Y. The C- and the N-Terminal Regions of Glycoprotein 41 Ectodomain Fuse Membranes Enriched and Not Enriched with Cholesterol, Respectively. *J. Biol. Chem.* **2004**, *279*, 18526−18534.
(47) Salzwedel, K.; West, J. T.; Hunter, E. A Conserved Tryptophan-Rich Motif in the Membrane-Proximal Region of the Human Immunodeficiency Virus Type 1 Gp41 Ectodomain Is Important for Env-Mediated Fusion and Virus Infectivity. *J. Virol.* **1999**, *73*, 2469−2480.
(48) Perez-Berna, A. J.; Bernabeu, A.; Moreno, M. R.; Guillen, J.; Villalain, J. The Pre-Transmembrane Region of the Hcv E1 Envelope Glycoprotein: Interaction with Model Membranes. *Biochim. Biophys. Acta* **2008**, *1778*, 2069−2080.
(49) Lorizate, M.; Huarte, N.; Saez-Cirion, A.; Nieva, J. L. Interfacial Pre-Transmembrane Domains in Viral Proteins Promoting Membrane Fusion and Fission. *Biochim. Biophys. Acta* **2008**, *1778*, 1624−1639.
(50) Lorizate, M.; de la Arada, I.; Huarte, N.; Sanchez-Martinez, S.; de la Torre, B. G.; Andreu, D.; Arrondo, J. L.; Nieva, J. L. Structural Analysis and Assembly of the Hiv-1 Gp41 Amino-Terminal Fusion Peptide and the Pretransmembrane Amphipathic-at-Interface Sequence. *Biochemistry* **2006**, *45*, 14337−14346.
(51) Gouttenoire, J.; Castet, V.; Montserret, R.; Arora, N.; Raussens, V.; Ruysschaert, J. M.; Diesis, E.; Blum, H. E.; Penin, F.; Moradpour, D. Identification of a Novel Determinant for Membrane Association in Hepatitis C Virus Nonstructural Protein 4b. *J. Virol.* **2009**, *83*, 6257−6268.
(52) Gouttenoire, J.; Roingeard, P.; Penin, F.; Moradpour, D. Amphipathic Alpha-Helix Ah2 Is a Major Determinant for the Oligomerization of Hepatitis C Virus Nonstructural Protein 4b. *J. Virol.* **2010**, *84*, 12529−12537.
(53) Guillen, J.; Gonzalez-Alvarez, A.; Villalain, J. A Membranotropic Region in the C-Terminal Domain of Hepatitis C Virus Protein Ns4b Interaction with Membranes. *Biochim. Biophys. Acta* **2010**, *1798*, 327−337.
(54) White, S. H.; Wimley, W. C. Membrane Protein Folding and Stability: Physical Principles. *Annu. Rev. Biophys. Biomol. Struct.* **1999**, *28*, 319−365.
(55) Engelman, D. M.; Steitz, T. A.; Goldman, A. Identifying Nonpolar Transbilayer Helices in Amino Acid Sequences of Membrane Proteins. *Annu. Rev. Biophys. Biophys. Chem.* **1986**, *15*, 321−353.
(56) Hessa, T.; Meindl-Beinker, N. M.; Bernsel, A.; Kim, H.; Sato, Y.; Lerch-Bader, M.; Nilsson, I.; White, S. H.; von Heijne, G. Molecular Code for Transmembrane-Helix Recognition by the Sec61 Translocon. *Nature* **2007**, *450*, 1026−1030.
(57) Moon, C. P.; Fleming, K. G. Side-Chain Hydrophobicity Scale Derived from Transmembrane Protein Folding into Lipid Bilayers. *Proc. Natl. Acad. Sci. U. S. A.* **2011**, *108*, 10174−10177.
(58) Koehler, J.; Woetzel, N.; Staritzbichler, R.; Sanders, C. R.; Meiler, J. A Unified Hydrophobicity Scale for Multispan Membrane Proteins. *Proteins* **2009**, *76*, 13−29.
(59) Eisenberg, D.; Weiss, R. M.; Terwilliger, T. C. The Helical Hydrophobic Moment: A Measure of the Amphiphilicity of a Helix. *Nature* **1982**, *299*, 371−374.
(60) Epand, R. M.; Hui, S. W. Effect of Electrostatic Repulsion on the Morphology and Thermotropic Transitions of Anionic Phospholipids. *FEBS Lett.* **1986**, *209*, 257−260.
(61) Lewis, R. N.; McElhaney, R. N.; Pohle, W.; Mantsch, H. H. Components of the Carbonyl Stretching Band in the Infrared Spectra of Hydrated 1,2-Diacylglycerolipid Bilayers: A Reevaluation. *Biophys. J.* **1994**, *67*, 2367−2375.
(62) Blume, A.; Hubner, W.; Messner, G. Fourier Transform Infrared Spectroscopy of 13c = O-Labeled Phospholipids Hydrogen Bonding to Carbonyl Groups. *Biochemistry* **1988**, *27*, 8239−8249.

(63) Arrondo, J. L.; Goni, F. M. Structure and Dynamics of Membrane Proteins as Studied by Infrared Spectroscopy. *Prog. Biophys. Mol. Biol.* **1999**, *72*, 367−405.
(64) Byler, D. M.; Susi, H. Examination of the Secondary Structure of Proteins by Deconvolved Ftir Spectra. *Biopolymers* **1986**, *25*, 469−487.
(65) Palomares-Jerez, M. F.; Guillen, J.; Villalain, J. Interaction of the N-Terminal Segment of HCV Protein NS5A with Model Membranes. *Biochim. Biophys. Acta* **2010**, *1798*, 1212−1224.